

**Electron-drag effect in Si metal-oxide-semiconductor devices with thin oxide layers**

Boris Laikhtman

*The Racah Institute of Physics, The Hebrew University, Jerusalem, 91904, Israel*

Paul M. Solomon

*IBM Semiconductor Research and Development Center: Research Division, T.J. Watson Research Center, Yorktown Heights, New York 10598, USA*

(Received 11 May 2005; published 22 September 2005)

We study theoretically and experimentally the electron-drag effect in silicon metal-oxide-semiconductor field-effect transistors with thin oxide layers. According to a former theoretical prediction the drag effect had to be significantly enhanced by the plasma resonance. However, recent experiments of Solomon and Yang did not confirm this prediction. We show that under the experimental conditions (the doping of the gate  $10^{19} \text{ cm}^{-3}$  and more) and room temperature the decay of plasma waves appears to be large and smears the resonance. The electron scattering in the gate is so strong that the energy uncertainty is larger than the temperature and regular microscopic transport theory for gate electrons cannot be used. For the calculation of the drag effect we make use of the method of correlators and describe transport in the gate with the help of phenomenological parameters. This approach gives good agreement with the experiment.

DOI: [10.1103/PhysRevB.72.125338](https://doi.org/10.1103/PhysRevB.72.125338)

PACS number(s): 73.40.-c, 72.10.-d, 85.30.Tv

**I. INTRODUCTION**

The drag effect was first observed by Solomon *et al.*<sup>1</sup> between two-dimensional (2D) and 3D electron gases and Gramila *et al.*<sup>2</sup> between two 2D electron gases. Since that time, the drag effect has been measured between two 2D electron gases,<sup>3-6</sup> between two 2D hole gases,<sup>7,8</sup> and between 2D electron and hole gases.<sup>9,10</sup> There were also a number of measurements of the drag between two 2D electron gases in magnetic field.<sup>10,11</sup> Recently it became clear that the effect is important not only for the study of the physics of interacting electron layers but also for applications.

The physical origin of the drag effect is the interaction between electrons in different layers that leads to electron momentum transfer between the layers.<sup>12,13</sup> Flensberg and Hu noticed that the electron-electron scattering probability proportional to  $V^2(q)/\epsilon(\omega, q)$ , where  $V(q)$  is bare Coulomb interaction between different layers and  $\epsilon(\omega, q)$  is the inter-layer dielectric function, could be very large near plasmon resonances where  $\epsilon(\omega, q)$  is zero.<sup>14</sup> The corresponding enhancement of the drag effect has been confirmed experimentally.<sup>15,16</sup> Fischetti and Laux calculated the channel electron mobility in Si metal-oxide-semiconductor (MOS) devices, taking into account scattering of channel electrons by gate electrons. They found significant degradation of the mobility for oxide thicknesses below  $\sim 2-3$  nm and ascribed this degradation to resonant scattering by surface plasmons<sup>17,18</sup> However, in recent experiments Solomon and Yang did not find any enhancement of the drag effect in Si MOS devices with thin oxide layers.<sup>19</sup> The experimental value of the channel-gate electron relaxation rate appeared by about two orders of magnitude smaller than calculated in Ref. 18.

The purpose of the present paper is to point out the physical reason for this discrepancy and to demonstrate that an adequate description of the electron gas leads to a correct estimate of the drag effect.

To understand the physical reason for the discrepancy it is necessary to check the applicability of the theoretical results to the experiment. Strong plasma resonance leading to a significant enhancement of the drag effect implies a weak decay of plasma waves. In other words, the imaginary part of the plasma frequency  $\omega(q)$  is small,  $\text{Im } \omega(q)/|\omega(q)| \ll 1$ . This condition is met in an electron gas with weak scattering. The situation in Si MOS devices typically is quite different. Specifically, in the experiment of Solomon and Yang<sup>19</sup> the gate was polycrystalline with the size of grains  $a_{gr} \approx 5$  nm. It was doped above  $10^{19} \text{ cm}^{-3}$ , and measurements were performed at room temperature. At this doping and temperature the electron mobility in crystalline Si,  $\mu_{cr} \approx 80 \text{ cm}^2/(\text{V s})$ , and is very weakly dependent on doping.<sup>20,21</sup> This corresponds to the relaxation time  $\tau_g = 1.5 \times 10^{-14}$  s, so that the energy uncertainty  $\hbar/\tau_g = 44$  meV is larger than the temperature and of the order or larger than the Fermi energy (for three samples of four,  $E_F$  varied from 17 meV to 48 meV and in the fourth sample it was around 98 meV). The same relation can be written as  $k_F l_g \lesssim 1$  where  $k_F$  is the Fermi wave vector and  $l_g$  is the mean free path. That is, even if the scattering is elastic or quasielastic, it changes the electron wave functions so dramatically that the wave vector uncertainty is larger or of the order of the wave vector itself, and the gate electron system cannot be considered as a free electron gas. The scattering by grain boundaries can only increase the wave vector uncertainty. That is, results obtained in the gas approximation<sup>14,17,18</sup> are not applicable in this case.

Contrary to this, the gas approximation is valid for channel electrons. Therefore the dissipation of surface plasmons originated from the channel is small. But this situation changes at small oxide thicknesses—i.e., exactly at region of parameters when plasmons can substantially affect the drag. If the separation between the channel and gate is of the order of or smaller than the characteristic plasmon wavelength, the whole plasma spectrum is strongly modified by the interac-

tion between gate and channel electrons. In this case the condition  $\text{Im } \omega(q)/|\omega(q)| \ll 1$  is not met for any branch of the spectrum and the plasmon enhancement of the drag effect does not take place.

Unfortunately, for the calculation of the drag effect in Si MOS devices we cannot make use of existing theoretical results. First calculations of the drag effect used the Boltzmann approximation.<sup>22–25</sup> Later the transconductivity and scattering rate between electron systems were expressed in the susceptibilities of the systems.<sup>9,26–32</sup> Although for further calculations the Coulomb interaction was taken sometimes beyond the random phase approximation (RPA),<sup>33,34</sup> in many works the susceptibilities were calculated still in the gas approximation.<sup>9,26–28,34,35</sup> For the consideration of strong impurity scattering the susceptibilities were calculated in the diffusion regime,<sup>29–32</sup> which is also not valid when  $\hbar/\tau$  is of the order of the Fermi energy.

To circumvent this problem and to avoid uncontrollable approximations we use a phenomenological approach. First we obtain an expression for the scattering rate of channel electrons by gate electrons in terms of the gate response function with the help of the method of correlators.<sup>36</sup> Then we calculate the response function in terms of the bulk phenomenological parameters—the conductivity and diffusion coefficients—which are measurable experimentally. The result of this approach appeared to be rather successful. We obtained the magnitude of the drag effect and its behavior versus the channel concentration close to the experiment.

It is necessary to emphasize that good agreement between the theory and experiment appeared in spite of some inaccuracy of the transport description in the gate. Inaccuracies are unavoidable due to lack of the transport theory in polycrystalline Si. The grain boundary trapping model developed for polycrystalline films contains adjustable parameters depending of details of the technology.<sup>37</sup> Also this model reasonably describes only dc mobility while for the calculation of electron-electron scattering it is necessary to know also the dispersion of the mobility when the transferred wave vector changes from values larger than the inverse size of the grains  $1/a_{gr}$  to values smaller than  $1/a_{gr}$ . The development of an adequate theory of the polycrystalline films is beyond the scope of the present work, and in our calculation we introduced mobility dispersion phenomenologically.

The paper is organized in the following way. In the next section we calculate the plasmon spectrum in a simplified model of a field-effect transistor (FET) and show that it is quite different in the cases of free and strongly scattered electrons in the gate. In Sec. III we calculate the scattering rate of channel electrons by the gate, and in Sec. IV we compare the theoretical and experimental results.

## II. PLASMA SPECTRUM IN FIELD EFFECT TRANSISTORS

In this section we calculate the plasma spectrum in a simplified model of the field-effect transistor. Our purpose is to study the dependence of the spectrum on the separation between the channel and gate and modification of the spectrum when electron scattering in the gate becomes strong.

We consider a system that consists of a two-dimensional conducting layer  $z=a$  (channel) and a conducting half-space  $z<0$  (gate) separated by an insulator. For simplicity we assume (in this section only) that the dielectric constant  $\kappa$  is the same in all conductors and insulators ( $0<z<a$  and  $z>a$ ). We are interested in the long-wavelength part of the spectrum and use the hydrodynamic approximation. That is, the dynamics of the 2D electron gas is described by the equations

$$\frac{\partial N}{\partial t} + N_0 \nabla_{\parallel} \mathbf{V} = 0, \quad (2.1a)$$

$$m \frac{\partial \mathbf{V}}{\partial t} = -\nabla_{\parallel} \left( e \phi(\mathbf{r}_{\parallel}, a) + \frac{d\zeta_c}{dN_0} N \right), \quad (2.1b)$$

where  $N_0$  and  $N$  are the equilibrium and nonequilibrium sheet electron concentrations,  $\mathbf{V}$  is the electron velocity,  $\zeta_c$  is the chemical potential,  $\phi(\mathbf{r}_{\parallel}, z)$  is the electric potential,  $m$  is the electron mass, and  $\mathbf{r}_{\parallel}$  is the in-plane coordinate.

For any gate model its response can be presented by the boundary conditions for the potential at the interface between the gate and insulator. After the Fourier transformation with respect to time and  $\mathbf{r}_{\parallel}$  this condition has the form

$$\left. \frac{d\phi_q}{dz} \right|_{z=0} = q[1 + \Lambda(\omega, q)]\phi_q(0). \quad (2.2)$$

Here  $\Lambda(\omega, q)$  is the response of the gate electron system that depends on the frequency  $\omega$  and wave vector  $q$ . If the gate is insulating, then  $\Lambda(\omega, q)=0$ .

The electric potential satisfies the Laplace equations in the regions  $0<z<a$  and  $z>a$ . It is continuous at  $z=a$  but its derivatives with respect to  $z$  satisfy the condition

$$\left. \frac{d\phi_q}{dz} \right|_{z=a+0} - \left. \frac{d\phi_q}{dz} \right|_{z=a-0} = -\frac{4\pi e}{\kappa} N_q. \quad (2.3)$$

The solution of Eqs. (2.1)–(2.3) together with the Laplace equation leads to the dispersion relation

$$\left( \omega^2 - gq - \frac{gq^2}{q_s} \right) [2 + \Lambda(\omega, q)] = -gq\Lambda(\omega, q)e^{-2qa}, \quad (2.4)$$

where

$$g = \frac{2\pi e^2 N_0}{\kappa m}, \quad q_s = \frac{2\pi e^2}{\kappa} \frac{dN_0}{d\zeta_c}. \quad (2.5)$$

If the plasmon wavelength is much shorter than the separation between the channel and gate,  $qa \gg 1$ , then Eq. (2.4) breaks down into the dispersion relation for surface waves and gate waves,

$$\omega^2 = gq + \frac{gq^2}{q_s}, \quad (2.6a)$$

$$\Lambda(\omega, q) = -2. \quad (2.6b)$$

For longer wavelengths,  $qa \lesssim 1$ , the surface and gate waves are strongly intermixed and to study the spectrum in

this case we consider two different models of the gate.

### A. Free electron gas

In this case the hydrodynamic approximation leads to the equations

$$\nabla^2 \phi = -\frac{4\pi e}{\kappa} n, \quad (2.7a)$$

$$\frac{\partial n}{\partial t} + n_0 \nabla \cdot \mathbf{v} = 0, \quad (2.7b)$$

$$m \frac{\partial \mathbf{v}}{\partial t} = -\nabla \left( e\phi + \frac{d\xi_g}{dn_0} n \right), \quad (2.7c)$$

with the boundary condition

$$v_z(\mathbf{r}_{\parallel}, 0) = 0. \quad (2.8)$$

Here  $n_0$  is the equilibrium electron concentrations,  $n$  is the deviation of the concentration from  $n_0$ ,  $\mathbf{v}$  is the electron velocity, and  $\xi_g$  is the chemical potential. The solution of these equations results in

$$\Lambda(\omega, q) = \frac{(1 + R_D^2 q^2 - \omega^2/\omega_p^2)^{1/2} - qR_D}{qR_D - (\omega^2/\omega_p^2)(1 + R_D^2 q^2 - \omega^2/\omega_p^2)^{1/2}}, \quad (2.9)$$

where

$$R_D = \left( \frac{\kappa}{4\pi e^2} \frac{d\xi_g}{dn_0} \right)^{1/2}, \quad \omega_p = \left( \frac{4\pi e^2 n_0}{\kappa m} \right)^{1/2} \quad (2.10)$$

are the Debye screening radius and bulk plasma frequency, respectively.

For small values of the wave vector,  $qR_D \ll 1$  and  $gq \ll \omega_p^2$ , Eqs. (2.4) and (2.9) lead to the following two branches of spectrum:

$$\omega^2 = \frac{\omega_p^2}{2} + gqe^{-2qa}, \quad (2.11a)$$

$$\omega^2 = gq \left( 1 - e^{-2qa} + \frac{q}{q_s} \right). \quad (2.11b)$$

The first branch is the gate wave with the limit frequency  $\omega_p/\sqrt{2}$ . The second branch behaves as an acoustic wave,  $\omega = q\sqrt{2ga(1+1/2aq_s)}$ , when the wavelength is larger than the separation between the gate and channel,  $qa \ll 1$ , and becomes the channel surface wave,  $\omega = \sqrt{gq(1+q/q_s)}$ , in the opposite case  $qa \gg 1$ . This spectrum has been obtained by Fischetti.<sup>18</sup>

### B. Strong electron scattering

In the case of strong scattering the electron transport in the gate can be described phenomenologically,

$$\nabla^2 \phi = -\frac{4\pi e}{\kappa} n, \quad (2.12a)$$

$$e \frac{\partial n}{\partial t} + \nabla \cdot \mathbf{j} = 0, \quad (2.12b)$$

$$\mathbf{j} = -\sigma \nabla \left( \phi + \frac{1}{e} \frac{d\xi}{dn_0} n \right), \quad (2.12c)$$

where  $\sigma$  is the conductivity and electric current  $\mathbf{j}$  satisfies the boundary condition

$$j_z(\mathbf{r}_{\parallel}, 0) = 0. \quad (2.13)$$

The solution of Eqs. (2.12) and (2.13) results in

$$\Lambda(\omega, q) = \frac{\sqrt{1 + q^2 R_D^2 - i\omega\tau_M} - qR_D}{qR_D - i\omega\tau_M \sqrt{1 + q^2 R_D^2 - i\omega\tau_M}}, \quad (2.14)$$

where

$$\tau_M = \frac{\kappa}{4\pi\sigma} \quad (2.15)$$

is the Maxwell relaxation time.

The spectrum is a complicated mixture of bulk waves and surface waves. Nonzero  $\text{Im} \Lambda(\omega, q)$  leads to a decay of all plasma waves. The decay of surface waves is suppressed only at the short-wavelength part of the spectrum,  $qa \gg 1$ , when the interaction between 2D gas and bulk electrons becomes small; see Eq. (2.6).

To make the picture more clear in the other case we consider wave vectors so small that  $qR_D \ll 1$  and  $q/q_s \ll 1$ . Then Eqs. (2.4) and (2.14) give

$$(\omega^2 - gq) \left( 2 + \frac{i}{\omega\tau_M} \right) + \frac{igq}{\omega\tau_M} e^{-2qa} = 0. \quad (2.16)$$

One of the branches of this spectrum is the charge spreading in the gate. The corresponding frequency  $\omega = -i/2\tau_M$  at very small  $q$  ( $gq \ll 1$ ) and very large  $q$  ( $qa \gg 1$ ), and it has a small dispersion in intermediate  $q$ . The other branch becomes the surface wave when  $qa \gg 1$  and decaying acoustic wave when  $qa \ll 1$ . When  $q$  goes to zero—i.e.,  $qa \ll 1$  and  $\omega\tau_M \ll 1$ —its dispersion relation becomes

$$\omega = (\sqrt{2ga - g^2\tau_M^2} - ig\tau_M)q. \quad (2.17)$$

In general, the decay of this branch depends on a few parameters and we estimate it for parameters relevant to the drag effect. For gate doping  $n_g = 10^{19} \text{ cm}^{-3}$  and dielectric constant  $\kappa = 11.9$  the Maxwell time  $\tau_M = 8 \times 10^{-15} \text{ s}$ . The relevant frequency is determined by the energy transfer in electron-electron scattering—i.e., temperature. At room temperature  $\omega \approx 4 \times 10^{13} \text{ s}^{-1}$  and  $\omega\tau_M \approx 0.3$ . The relevant wave vector  $q$  is around the transferred wave vector that is of the order of the channel thermal wave vector (at room temperature the electron degeneracy in the channel is very weak even at high sheet concentration). The electron mass in the channel is the light electron mass  $m_{el} = 0.19$ , which gives  $q \sim 3.7 \times 10^6 \text{ cm}^{-1}$ . That is, at  $a \sim 2-3 \text{ nm}$ ,  $qa \sim 1$  and  $\text{Im} \omega/\text{Re} \omega \sim \tau_M \sqrt{g/a}$ . At  $N_0 = 10^{12} \text{ cm}^{-2}$  we have  $g = 7 \times 10^{20} \text{ cm/s}^2$ , which leads to  $\text{Im} \omega/\text{Re} \omega \sim 0.4$ . At higher channel concentration this ratio is larger.

That is, we come to the conclusion that it is hardly possible to expect the plasmon enhancement of the drag effect in silicon MOSFET's at room temperature.

### III. DRAG IN SILICON MOSFET'S

To develop the theory of the drag effect we consider the situation when an external source supports an electric current in the gate and a secondary drag current is induced in the channel. Then the drag current is controlled by the electron momentum relaxation time in the channel due to the interaction with the gate,  $\tau_{cg}$ , and the main purpose of this section is to derive an expression for this relaxation time. In Sec. III A we obtain an expression for  $\tau_{cg}$  in terms of the linear response of the system that comprise the barrier and gate. The dielectric constants of the barrier and gate are strongly different, which complicates the solution of the electrostatic problem necessary for the calculation of the response function. In Sec. III B we present the results of this solution, which gives an expression of the linear response function in the polarizability of the channel and gate. With the help of these expressions we obtain the final expression for the channel-gate momentum relaxation rate in Sec. III C.

#### A. Momentum relaxation time in the channel

The conduction band of Si consists of six strongly anisotropic valleys that are characterized by heavy electron mass  $m_{eh}=0.98$  and light electron mass  $m_{el}=0.19$ . For two valleys the axis with the heavy electron mass is directed normally to the Si/SiO<sub>2</sub> interface, and for the other four valleys the mass in the direction normal to the Si/SiO<sub>2</sub> interface is  $m_{el}$ . Due to size quantization in the channel, the valleys with in-plane heavy electron masses are shifted in energy above the other two valleys by  $\delta E$ . The acceptor concentration in the substrate in the experiment was  $n_A=4 \times 10^{17} \text{ cm}^{-3}$ . For this  $n_A$  and channel concentration  $n_c=10^{12} \text{ cm}^{-2}$  the variational calculation<sup>38</sup> gives  $\delta E=71 \text{ meV}$ . For such a high-energy separation the occupation of the higher valleys is small in spite of a large density of states there, and we neglect this occupation. Because of the inaccuracy of the transport description in the polycrystalline gate that we mentioned in the Introduction, the corrections coming from the higher valley occupation are beyond the precision of our calculation. The in-plane spectrum of the two occupied valleys is isotropic with effective mass  $m_{el}$ .

The electron momentum relaxation time in the channel due to the interaction with the gate is defined by the relation

$$\left(\frac{d\mathbf{P}_c}{dt}\right)_{gc} = -\frac{1}{\tau_{cg}}\mathbf{P}_c, \quad (3.1)$$

where

$$\mathbf{P}_c = 4\hbar \int \mathbf{k} f_{\mathbf{k}} \frac{d\mathbf{k}}{(2\pi)^2} \quad (3.2)$$

is the density of the electron momentum in the channel. The extra factor of 2 in Eq. (3.2) comes from two equivalent valleys contributing to the total momentum.

The left-hand side of Eq. (3.1) can be calculated with the help of the collision integral,

$$\left(\frac{\partial f_{\mathbf{k}}}{\partial t}\right)_{cg} = \int [W_{\mathbf{k}' \rightarrow \mathbf{k}} f_{\mathbf{k}'}(1-f_{\mathbf{k}}) - W_{\mathbf{k} \rightarrow \mathbf{k}'} f_{\mathbf{k}}(1-f_{\mathbf{k}'})] \frac{d\mathbf{k}'}{(2\pi)^2}, \quad (3.3)$$

Here intervalley transitions are neglected because they require the transferred wave vector  $q \geq \pi\sqrt{2}/a_0 \approx 8 \times 10^7 \text{ cm}^{-1}$  where  $a_0=5.43 \text{ \AA}$  is the Si lattice constant. It is well known that the momentum transfer between the channel and gate is suppressed by the factor  $e^{-qa}$  in the transition probability, where  $a$  is the thickness of the oxide layer separating the gate and channel [see Refs. 22–25, 28, and 29 and Eqs. (3.19), (3.20), and (3.24) below]. For  $a \geq 1 \text{ nm}$  this factor is smaller than  $3 \times 10^{-4}$ .

The electron transition probability per unit time from the state with wave vector  $\mathbf{k}$  to the state with wave vector  $\mathbf{k}'$  meets the detail balance condition

$$W_{\mathbf{k}' \rightarrow \mathbf{k}} = e^{(E_{\mathbf{k}'} - E_{\mathbf{k}})/T} W_{\mathbf{k} \rightarrow \mathbf{k}'}. \quad (3.4)$$

Hereafter we assume that the electrons in the gate and channel have the same temperature  $T$ . After the substitution of Eqs. (3.2) and (3.3) on the left-hand side of Eq. (3.1), a couple of substitutions  $\mathbf{k} \rightleftharpoons \mathbf{k}'$ , and the help of Eq. (3.4) it is reduced to the form

$$\left(\frac{d\mathbf{P}_c}{dt}\right)_{gc} = 4 \int \frac{d\mathbf{k}}{(2\pi)^2} \frac{d\mathbf{k}'}{(2\pi)^2} (\mathbf{k}' - \mathbf{k}) f_{\mathbf{k}}(1-f_{\mathbf{k}'}) W_{\mathbf{k} \rightarrow \mathbf{k}'}. \quad (3.5)$$

The distribution function in the channel can be taken in the drift approximation,

$$f_{\mathbf{k}} = f_0(E_{\mathbf{k}} - \hbar\mathbf{k}\mathbf{V}) \approx f_0(E_{\mathbf{k}}) - \hbar\mathbf{k}\mathbf{V}f_0'(E_{\mathbf{k}}), \quad (3.6)$$

where  $f_0(E)$  is the Fermi function. The drift approximation is justified because a rough estimate for the electron-electron relaxation time in the channel gives  $10^{-13} \text{ s}$ , which is shorter than the relaxation time due to other scattering mechanisms. The substitution of Eq. (3.6) into Eq. (3.2) gives

$$\mathbf{P} = n_c m_{el} \mathbf{V}. \quad (3.7)$$

The substitution of Eq. (3.6) into Eq. (3.5) leads to

$$\left(\frac{d\mathbf{P}_c}{dt}\right)_{gc} = \frac{2\hbar^2}{T} \int \frac{d\mathbf{k}}{(2\pi)^2} \frac{d\mathbf{k}'}{(2\pi)^2} (\mathbf{k}' - \mathbf{k}) [(\mathbf{k}\mathbf{V}) - (\mathbf{k}'\mathbf{V})] f_0(E_{\mathbf{k}}) \times [1 - f_0(E_{\mathbf{k}'})] W_{\mathbf{k} \rightarrow \mathbf{k}'}. \quad (3.8)$$

Due to the isotropy of the in-plane spectrum,  $W_{\mathbf{k} \rightarrow \mathbf{k}'}$  depends only on  $k, k'$  and the angle between  $\mathbf{k}$  and  $\mathbf{k}'$ . Then Eq. (3.8) can be reduced to the form (3.1) (see the Appendix) where

$$\frac{1}{\tau_{cg}} = \frac{\hbar^2}{T m_{el} n_c} \int \frac{d\mathbf{k}}{(2\pi)^2} \frac{d\mathbf{k}'}{(2\pi)^2} (\mathbf{k}' - \mathbf{k})^2 f_0(E_{\mathbf{k}}) \times [1 - f_0(E_{\mathbf{k}'})] W_{\mathbf{k} \rightarrow \mathbf{k}'}. \quad (3.9)$$

Now it is necessary to find the transition probability  $W_{\mathbf{k} \rightarrow \mathbf{k}'}$ .

There are two main mechanisms of the interaction between electrons in the channel and electrons in the gate, Coulomb interaction,<sup>12,13,22–24,26</sup> and exchange by virtual phonons.<sup>3,26,39</sup> The coupling constant of the phonon exchange is smaller, and this mechanism is important in the cases when the Coulomb interaction is suppressed—e.g., at the very thick insulator between the channel and gate (the Coulomb interaction falls off with distance much faster than the phonon exchange).<sup>26,39</sup> In Si MOS devices with thin oxide layers there is no reason for the suppression of the Coulomb interaction and an estimate made with the help of Ref. 39 shows that the phonon exchange is smaller than the Coulomb interaction by more than two orders of magnitude.

For the derivation of the transition probability we make use of method of correlators<sup>36</sup> that have been applied to the drag problem by Maslov.<sup>24</sup> Channel electrons are scattered by fluctuations of the electric potential produced by the gate electrons, and the transition probability can be expressed in the correlation function of the electric potential,

$$K(\mathbf{r}_{\parallel 1} - \mathbf{r}_{\parallel 2}, z_1, z_2, t_1 - t_2) = \text{Tr}[\hat{\rho} \hat{\phi}(\mathbf{r}_{\parallel 1}, z_1, t_1) \hat{\phi}(\mathbf{r}_{\parallel 2}, z_2, t_2)], \quad (3.10)$$

where  $\hat{\rho}$  is the density matrix,  $\hat{\phi}(\mathbf{r}_{\parallel}, z, t)$  is the operator of the electric potential,  $z$  is the coordinate in the direction normal to Si/SiO<sub>2</sub> interface, and  $\mathbf{r}_{\parallel}$  is the in-plane coordinate. The transition probability is connected to the correlation function by the relation

$$W_{\mathbf{k} \rightarrow \mathbf{k}'} = \frac{e^2}{\hbar^2} K(\mathbf{k}' - \mathbf{k}, (E_{\mathbf{k}'} - E_{\mathbf{k}})/\hbar), \quad (3.11)$$

where

$$K(\mathbf{q}, \omega) = \int dz_1 \int dz_2 \zeta^2(z_1) \zeta^2(z_2) \times \int_{-\infty}^{\infty} e^{i\omega t} dt \int e^{-i\mathbf{q}\cdot\mathbf{r}_{\parallel}} K(\mathbf{r}_{\parallel}, z_1, z_2, t), \quad (3.12)$$

and  $\zeta(z)$  is the wave function of the channel electrons.

According to the fluctuation-dissipation theorem, the correlation function of the potential is expressed in the linear response function that describes the electric potential induced by a perturbation of the electron concentration,

$$K(\mathbf{q}, \omega) = - \frac{2\hbar}{e^{\hbar\omega/T} - 1} \text{Im } \mathcal{D}(\omega, \mathbf{q}). \quad (3.13)$$

Substitution of Eqs. (3.11) and (3.13) into Eq. (3.9) leads to

$$\frac{1}{\tau_{cg}} = - \frac{2\hbar e^2}{T m_e \mu_c} \int \frac{d\mathbf{k}}{(2\pi)^2} \frac{d\mathbf{q}}{(2\pi)^2} q^2 f_0(E_{\mathbf{k}}) \times [1 - f_0(E_{|\mathbf{k}+\mathbf{q}|})] \frac{\text{Im } \mathcal{D}(\omega, \mathbf{q})}{e^{\hbar\omega/T} - 1}, \quad (3.14)$$

where  $\hbar\omega = E_{|\mathbf{k}+\mathbf{q}|} - E_{\mathbf{k}}$ .

## B. Linear response function

We consider the geometry when the polysilicon gate occupies the region  $z < 0$ , the channel is formed in the crystalline Si in the region  $z > a$ , and the region  $0 < z < a$  is occupied by a SiO<sub>2</sub> barrier. The dielectric constant of the Si substrate ( $z > a$ ) and gate,  $\kappa = 11.9$ , is different from the dielectric constant of the barrier,  $\kappa_1$ . The linear response function of the channel in the presence of the gate has to be found from the solution to the electrostatic problem that includes the polarization of the channel and gate electrons. Following standard notation we write it in the form

$$\mathcal{D}(\omega, \mathbf{q}) = \frac{\mathcal{D}_0(\mathbf{q})}{\epsilon(\omega, \mathbf{q})}, \quad (3.15)$$

where  $\mathcal{D}_0(\mathbf{q})$  is the linear response in the channel without screening by the channel and gate electrons and  $\epsilon(\omega, \mathbf{q})$  is the dielectric function that comes from the polarizability of the channel electrons,

$$F(\omega, \mathbf{q}) = - \frac{8\pi e^2}{\kappa q} \int \frac{f_0(E_p) - f_0(E_{|p-\mathbf{q}|})}{\hbar\omega - E_{|p-\mathbf{q}|} + E_p + i\delta} \frac{d^2\mathbf{p}}{(2\pi)^2}, \quad (3.16)$$

and the gate electrons. The polarizability of the gate is introduced with the help of a boundary condition similar to Eq. (2.2), which is modified due to different dielectric constants in the barrier and gate,

$$\left. \frac{d\phi_q}{dz} \right|_{z=0} = \frac{\kappa}{\kappa_1} q [1 + \Lambda(\omega, \mathbf{q})] \phi_q(0). \quad (3.17)$$

Electron scattering in the gate is very strong, and transport there is described phenomenologically, Sec. II B, which leads to Eq. (2.14) for  $\Lambda(\omega, \mathbf{q})$ .

As a result,

$$\mathcal{D}_0(\mathbf{q}) = \frac{2\pi}{\kappa q} d_1(\mathbf{q}), \quad (3.18a)$$

$$\epsilon(\omega, \mathbf{q}) = \frac{1 + d_1(\mathbf{q})F(\omega, \mathbf{q}) + \frac{g_0(\mathbf{q})}{g(\mathbf{q})} \frac{\kappa}{\kappa_1} \Lambda(\omega, \mathbf{q}) + d_2(\mathbf{q})F(\omega, \mathbf{q})\Lambda(\omega, \mathbf{q})}{1 + \frac{d_2(\mathbf{q})}{d_1(\mathbf{q})} \Lambda(\omega, \mathbf{q})}, \quad (3.18b)$$

where

$$d_1(q) = H(q) + 2 \left( \frac{\kappa^2}{\kappa_1^2} - 1 \right) \frac{\Delta^2(q)}{g(q)} \sinh qa, \quad (3.19a)$$

$$d_2(q) = \frac{g_0(q)}{g(q)} \frac{\kappa}{\kappa_1} d_1(q) - 2 \left[ \frac{2\Delta(q)}{g(q)} \frac{\kappa}{\kappa_1} \right]^2 \quad (3.19b)$$

and

$$g(q) = \left( 1 + \frac{\kappa}{\kappa_1} \right)^2 e^{qa} - \left( 1 - \frac{\kappa}{\kappa_1} \right)^2 e^{-qa}, \quad (3.20a)$$

$$g_0(q) = \left( 1 + \frac{\kappa}{\kappa_1} \right) e^{qa} + \left( 1 - \frac{\kappa}{\kappa_1} \right) e^{-qa}. \quad (3.20b)$$

To calculate the channel form factors  $H(q)$  and  $\Delta(q)$  we make use of the Fang-Howard variational function<sup>38,40</sup>

$$\zeta(z) = \sqrt{\frac{b^3}{2}} (z-a) e^{-b(z-a)/2}, \quad (3.21)$$

where  $b = (48\pi e^2 m_{hc} n^* / \kappa \hbar^2)^{1/3}$ ,  $n^* = n_d + 11n_c/32$ ,  $n_d = n_A z_d$  is the sheet concentration of the depletion layer,  $z_d = \sqrt{\kappa E_g / 2\pi e^2 n_A}$  is the width of the depletion layer, and  $E_g = 1.1$  eV is the Si band gap. This gives<sup>38</sup>

$$H(q) = \int_a^\infty e^{-q|z-z'|} \zeta^2(z) \zeta^2(z') dz dz' = \frac{b(8b^2 + 9bq + 3q^2)}{8(b+q)^3}, \quad (3.22a)$$

$$\Delta(q) = \int_a^\infty e^{-qz} \zeta^2(z) dz = \frac{b^3}{(b+q)^3}. \quad (3.22b)$$

### C. Final expression for $1/\tau_{cg}$

In the substitution of Eq. (3.15) into Eq. (3.14) one has to keep in mind that  $D_0(q)$  is real and the imaginary part of  $1/\epsilon(\omega, q)$  comes from two sources:  $\text{Im} F(\omega, q)$  and  $\text{Im} \Lambda(\omega, q)$ . Both  $\text{Im} F(\omega, q)$  and  $\text{Im} \Lambda(\omega, q)$  describe real

electron-electron collisions in the channel and gate, respectively. Substitution of the part of  $\text{Im}[1/\epsilon(\omega, q)]$  proportional to  $\text{Im} F(\omega, q)$  in Eqs. (3.13) and (3.15) and then into Eqs. (3.11) and (3.3) gives regular collision integral of the channel electrons that conserves the total momentum. For this reason the part of  $\text{Im}[1/\epsilon(\omega, q)]$  proportional to  $\text{Im} F(\omega, q)$  has to be omitted in the calculation of the channel momentum relaxation.<sup>24</sup> In the rest of  $\text{Im}[1/\epsilon(\omega, q)]$  the drift part of the channel electron distribution function, Eq. (3.6), can be neglected. That is the part that describes channel-gate electron-electron scattering is

$$\left[ \text{Im} \frac{1}{\epsilon(\omega, q)} \right]_{cg} = \frac{U_n(q) \text{Im} \Lambda(\omega, q)}{[1 + U_r(\omega, q)]^2 + U_i^2(\omega, q)}, \quad (3.23)$$

where

$$U_r(\omega, q) = d_1(q) \text{Re} F(\omega, q) + \frac{g_0(q)}{g(q)} \frac{\kappa}{\kappa_1} \text{Re} \Lambda(\omega, q) + d_2(q) \times [\text{Re} F(\omega, q) \text{Re} \Lambda(\omega, q) - \text{Im} F(\omega, q) \text{Im} \Lambda(\omega, q)], \quad (3.24a)$$

$$U_i(\omega, q) = d_1(q) \text{Im} F(\omega, q) + \frac{g_0(q)}{g(q)} \frac{\kappa}{\kappa_1} \text{Im} \Lambda(\omega, q) + d_2(q) \times [\text{Re} F(\omega, q) \text{Im} \Lambda(\omega, q) + \text{Im} F(\omega, q) \text{Re} \Lambda(\omega, q)], \quad (3.24b)$$

$$U_n(q) = \frac{2}{d_1(q)} \left[ \frac{2\Delta(q)}{g(q)} \frac{\kappa}{\kappa_1} \right]^2. \quad (3.24c)$$

Finally, with the help of the relation<sup>9,28,41</sup>

$$\text{Im} F(\omega, q) = \frac{8\pi^2 e^2}{\kappa q} (1 - e^{-\hbar\omega/T}) \times \int f_0(E_{|p-q}) \times [1 - f_0(E_p)] \delta(\hbar\omega - E_p + E_{|p-q}) \frac{d^2 p}{(2\pi)^2}, \quad (3.25)$$

we come to the result

$$\frac{1}{\tau_{cg}} = \frac{\hbar^2}{16\pi^2 T m_e n_c} \int_0^\infty q^3 dq \int_0^\infty d\omega \frac{d_1(q)}{\sinh^2(\hbar\omega/2T)} \frac{U_n(\omega, q)}{[1 + U_r(\omega, q)]^2 + U_i^2(\omega, q)} \times \text{Im} \Lambda(\omega, q) \text{Im} F(\omega, q). \quad (3.26)$$

## IV. RESULTS AND DISCUSSION

First of all we calculate the dependence of the channel-gate electron-electron scattering rate on the thickness of the  $\text{SiO}_2$  barrier. To avoid all nonrelevant effects we assume that the gate is crystalline. In Figs. 1(a) and 1(b) we present the results for two different channel concentrations. We see a regular decrease of the rate with the thickness that comes from the limitation of the wave vector transferred in

electron-electron collisions by the inverse distance between the gate and channel. There is no trace of any enhancement induced by the plasma resonance. The magnitude of the drag rate at  $a_{\text{SiO}_2} = 1$  nm is about 1000 times smaller than that calculated in Ref. 18 at the same channel and gate concentration.

Experimentally, the drag effect is characterized by the ratio of the current induced in the gate by the current in the

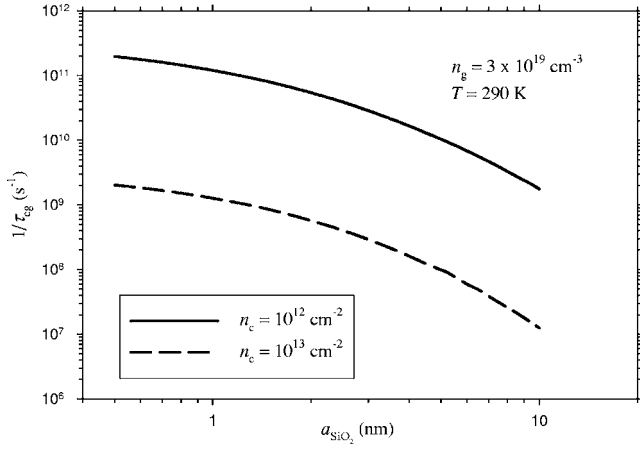


FIG. 1. The relaxation rate of channel electrons by gate electrons as a function of the oxide thickness for two different channel concentrations.

channel,  $A_I^{I_{gc}}$ . Making use of the momentum conservation this ratio can be expressed in the mobility ratio<sup>19</sup>

$$A_I = \frac{\mu_{poly}}{\mu_{cg}}, \quad (4.1)$$

where  $\mu_{cg} = e\tau_{cg}/m_{el}$ . In what follows we use the expression of  $\tau_{cg}$  obtained in Sec. III C for the calculation of  $A_I$  and compare the theoretical results with the experiment.

In the calculation of the drag rate  $1/\tau_{cg}$  we keep in mind that the gate voltage that controls the channel concentration creates also a depletion layer in the gate. We approximate the width of this layer as  $a_g = (n_c + n_d)/n_g$ , so that the total width of the layer separating the gate and channel is  $a = a_{SiO_2} + a_g$ , where  $a_{SiO_2}$  is the width of the  $SiO_2$  barrier. The effective dielectric constant  $\kappa_1$  of this layer is estimated as that corresponding to two capacitors (the  $SiO_2$  barrier and the gate depletion layer) connected in series,

$$\frac{a}{\kappa_1} = \frac{a_{SiO_2}}{\kappa_{SiO_2}} + \frac{a_g}{\kappa}, \quad (4.2)$$

where  $\kappa_{SiO_2} = 11.9$  and  $\kappa = 3.9$ .

Measurements were made on four types of samples that differed by the gate doping. The main characteristics of the samples are given in Table I. The gate mobility depended on the channel concentration  $n_c$ , and in the relevant region of the concentration was approximated by a linear function. The value of the diffusion coefficient in the gate,  $(\sigma/e^2)d\zeta/dn_0$ ,

is not known, so we do not have an experimental value of the screening radius. We calculated it with the help of its mean-field expression, Eq. (2.10).

The substitution of these data into the expression for  $\tau_{cg}$  gives results that differ from the experiment by about 50%–100%. This means that the main physical effects contributing to the drag are described correctly. We relate the remaining discrepancy to the polycrystalline structure of the gate that has not been taken into account in the calculation of  $\tau_{cg}$ . As we already mentioned in the Introduction, the transferred wave vector  $q$  changes from values larger than  $1/a_{gr}$  to values smaller than  $1/a_{gr}$  and this has to lead to a mobility dispersion from the crystal mobility  $\mu_{cr}$  at  $q \gg 1/a_{gr}$  to  $\mu_{poly}$  at  $q \ll 1/a_{gr}$ . The development of an adequate mobility theory in polycrystalline films is beyond the scope of the present work, and we approximated the mobility dependence on the wave vector as

$$\mu(q) = \mu_{cr} - \frac{\mu_{cr} - \mu_{poly}}{1 + C(qa_{gr})^2}, \quad (4.3)$$

where  $\mu_{cr}$  is the single-crystal mobility,  $\mu_{poly}$  is polycrystal mobility,  $a_{gr}$  is the size of the grains, and  $C$  is an adjustable parameter that depends on details of the technology.<sup>37</sup>

We compared the theoretical and experimental results only for sample A, B, and C. The doping of sample D is so high that the average distance between phosphorus donors, 1.8 nm, is of the order of the radius of its state, 1.2 nm.<sup>42</sup> Under this condition the band structure is distorted and there are no reliable values of the crystalline mobility and the screening radius.

Both theoretical and experimental values of the current ratio for samples A, B, and C are shown in Figs. 2(a) and 2(b) for two different thicknesses of the  $SiO_2$  barrier. The parameter  $C$  for the A, B, and C samples was 0.125, 0.0625, and 0.025, respectively. The matching is reasonable and the discrepancy is not surprising due to a rather rough description of the mobility dispersion in polycrystal.

To estimate how sensitive the results are to the exact value of the parameter  $C$  we calculated the current ratio for the chosen values of  $C$  for all the samples for the channel concentration  $n_c = 3 \times 10^{11} \text{ cm}^{-2}$ . The results are given in Table II. One can see that the variation of  $C$  can change the results by less than 40%. The difference between the cases of weak and strong electron scattering in the gate is more than two orders of magnitude, and the difference between the drag in devices with amorphous and crystalline gate, Fig. 3, is a few times. This confirms that our approach correctly describes the main features of the phenomena and the adjust-

TABLE I. Parameters of the samples.

	$n_g$ ( $\text{cm}^{-3}$ )	$E_F$ (meV)	$k_F$ ( $10^6 \text{ cm}^{-1}$ )	$R_D$ (nm)	$\mu_{poly}$ [ $\text{cm}^2/(\text{V s})$ ]
A	$1.2 \times 10^{19}$	17.5	2.9–6.7	1.26	$(2.7-0.15)n_c$
B	$2.8 \times 10^{19}$	40.2	4.5–10.2	0.89	$(5.3-0.10)n_c$
C	$5.6 \times 10^{19}$	81.4	6.4–14.5	0.70	$(5.1-0.08)n_c$
D	$16 \times 10^{19}$	227	10.6–24.1	0.54	$(4.1-0.11)n_c$

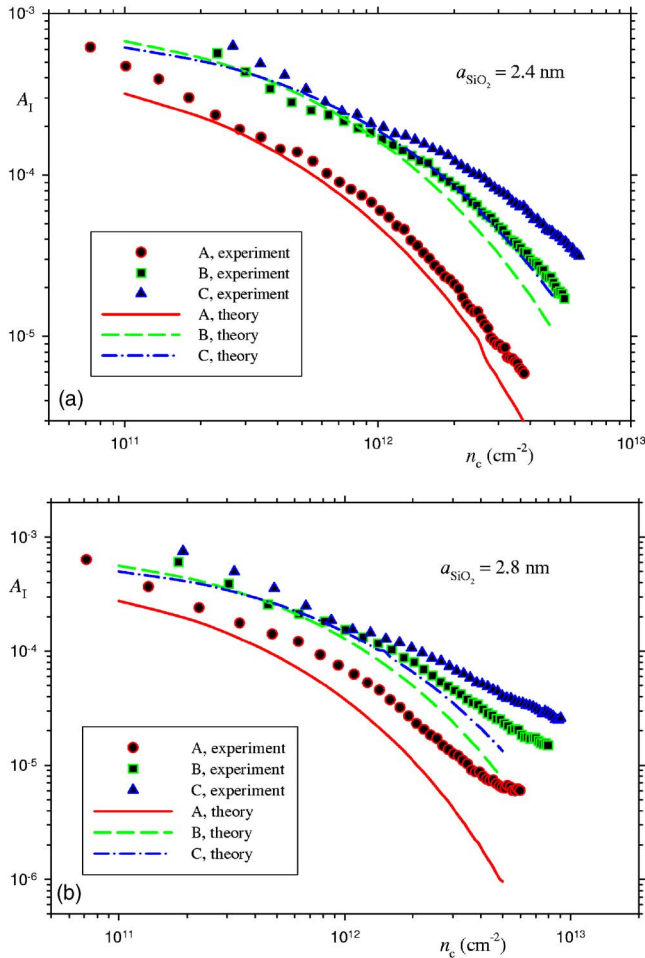


FIG. 2. (Color online) The ratio of the channel current to the gate current as function of the channel concentration for samples A, B, and C.

ment of C is only an attempt of a fine-tuning.

If the gate is crystalline, then the mobility becomes larger and it is easier to involve the gate electrons in motion. That is, one can expect an increase of the drag in devices with the crystalline gate compared to those with the polycrystalline gate. But the increase of the mobility leads also to a decrease of the Maxwell time and therefore to a decrease of the gate response  $\text{Im } \Lambda(\omega, q)$ . This effect decreases the drag. As a result the overall increase of the drag is significantly smaller than the ratio of the crystal and polycrystal mobilities. This can be seen from Fig. 3 where theoretical values of the current ratio for FET's with a crystalline gate and doping corre-

TABLE II. The current ratio for different values of the parameter C. Bold font marks the values for which C has been adjusted to fit better the experimental data. The channel concentration in all cases is  $n_c = 3 \times 10^{11} \text{ cm}^{-2}$ .

	C=0.125	C=0.0625	C=0.025
A	<b><math>1.74 \times 10^{-4}</math></b>	$1.85 \times 10^{-4}$	$1.94 \times 10^{-4}$
B	$3.79 \times 10^{-4}$	<b><math>4.35 \times 10^{-4}</math></b>	$4.89 \times 10^{-4}$
C	$2.91 \times 10^{-4}$	$3.58 \times 10^{-4}$	<b><math>4.31 \times 10^{-4}</math></b>

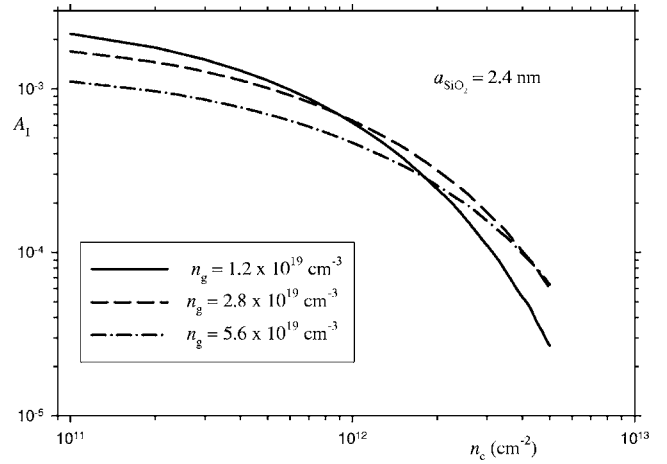


FIG. 3. Theoretical values of the current ratio for devices with crystalline gate. The increase of the current ratio compared to the polycrystalline gate is significantly smaller than the increase of the gate mobility.

sponding to samples A, B, and C are presented. Compared to the crystalline gate, Fig. 2(a), the current ratio in devices with a crystalline gate can increase from 2 times to the order of magnitude, depending on the gate doping and channel concentration. The increase is still not so big to reduce substantially the channel mobility. This is not surprising because according to the estimate given in the Introduction electron scattering for high doping is strong enough to suppress the plasmon resonance even in the crystalline gate.

In Fig. 4 we show the dependence of the current ratio on the thickness of SiO<sub>2</sub> barrier. This dependence is nearly exponential, and the characteristic length insignificantly grows with the gate concentration: it is approximately 2 nm, 1.7 nm, and 1.6 nm for samples A, B, and C, respectively.

In the last years there has been a lot of interest in materials with a high dielectric constant of the barrier that could replace SiO<sub>2</sub> as a barrier material and improve the perfor-

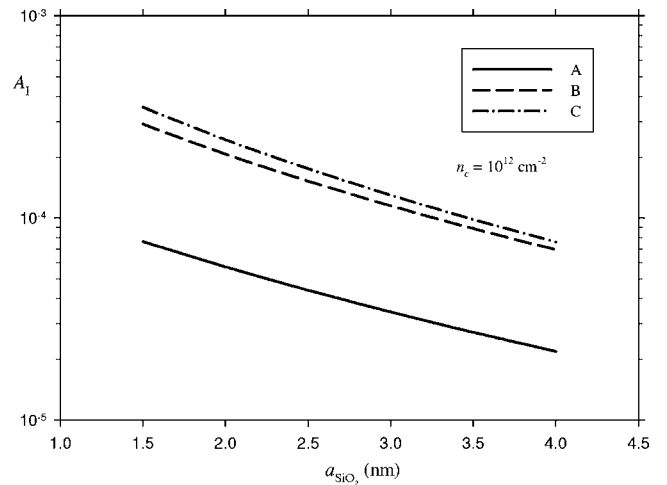


FIG. 4. The dependence of the current ratio on the thickness of the barrier. Reduction of the barrier thickness leads to an increase of the current ratio, but the ratio is saturated when the thickness becomes close or smaller than the electron wavelength.

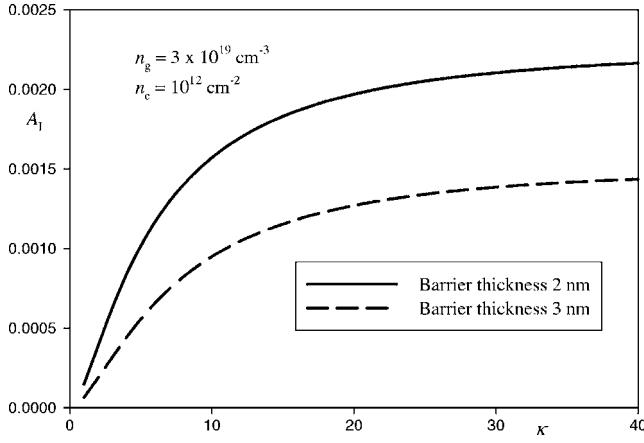


FIG. 5. The dependence of the current ratio on the dielectric constant of the barrier material. The gate is assumed to be crystalline.

mance of the device (see, e.g., Wilk *et al.*<sup>43</sup>). To meet such an interest we demonstrate in Fig. 5 the dependence of the current ratio on the dielectric constant of the barrier material for two different thicknesses of the barrier. The drag effect grows with the dielectric constant of the barrier and saturates when this dielectric constant becomes larger than the dielectric constant in the channel and gate.

## V. CONCLUSION

Analysis of the plasma spectrum in silicon MOSFET's with large gate doping shows a significant damping of plasma waves due to strong electron scattering in the gate. This damping eliminates the enhancement of the drag effect by plasma resonance that has been observed in other devices.<sup>15,16</sup> The correct estimate of the drag effect can be made with the help of a phenomenological description of electron transport in the gate. Such an approach results in a good matching between theoretical and experimental results.

## APPENDIX A: REDUCTION OF THE ANGULAR INTEGRALS

Equation (3.9) contains two types of angular integrals:

$$I_{1\alpha\beta} = \int_0^{2\pi} d\phi_k \int_0^{2\pi} d\phi_{k'} k_\alpha k_\beta u[\cos(\phi_k - \phi_{k'})], \quad (\text{A1a})$$

$$I_{2\alpha\beta} = \int_0^{2\pi} d\phi_k \int_0^{2\pi} d\phi_{k'} k_\alpha k'_\beta u[\cos(\phi_k - \phi_{k'})], \quad (\text{A1b})$$

where  $\phi_k$  and  $\phi_{k'}$  are the angles between the  $\mathbf{k}$  and  $\mathbf{k}'$  vectors, respectively, and  $x$  axis. In the first integral it is convenient first to integrate with respect to  $\phi_{k'}$ , and then the integrand, except the factor  $k_\alpha k_\beta$ , does not depend on the angle. As a result,

$$I_{1\alpha\beta} = \delta_{\alpha\beta} \frac{k^2}{2} \int_0^{2\pi} d\phi_k \int_0^{2\pi} d\phi_{k'} u[\cos(\phi_k - \phi_{k'})]. \quad (\text{A2})$$

The components of the second integral have to be considered separately:

$$\begin{aligned} I_{2xx} &= kk' \int_0^{2\pi} d\phi_k \int_0^{2\pi} d\phi_{k'} \cos \phi_k \cos \phi_{k'} u[\cos(\phi_k - \phi_{k'})] \\ &= \pi kk' \int_0^{2\pi} d\phi \cos \phi u(\cos \phi), \end{aligned} \quad (\text{A3a})$$

$$\begin{aligned} I_{2xy} &= kk' \int_0^{2\pi} d\phi_k \int_0^{2\pi} d\phi_{k'} \cos \phi_k \sin \phi_{k'} u[\cos(\phi_k - \phi_{k'})] \\ &= -\pi kk' \int_0^{2\pi} d\phi \sin \phi u(\cos \phi) = 0, \end{aligned} \quad (\text{A3b})$$

$$\begin{aligned} I_{2yy} &= kk' \int_0^{2\pi} d\phi_k \int_0^{2\pi} d\phi_{k'} \sin \phi_k \sin \phi_{k'} u[\cos(\phi_k - \phi_{k'})] \\ &= \pi kk' \int_0^{2\pi} d\phi \cos \phi u(\cos \phi). \end{aligned} \quad (\text{A3c})$$

That is,

$$I_{2\alpha\beta} = \delta_{\alpha\beta} \frac{1}{2} \int_0^{2\pi} d\phi_k \int_0^{2\pi} d\phi_{k'} k k' u[\cos(\phi_k - \phi_{k'})]. \quad (\text{A4})$$

As a result, the complete angular integral in Eq. (3.9) is

$$\begin{aligned} &\int_0^{2\pi} d\phi_k \int_0^{2\pi} d\phi_{k'} (k_\alpha - k'_\alpha)(k_\beta - k'_\beta) u[\cos(\phi_k - \phi_{k'})] \\ &= \delta_{\alpha\beta} \frac{1}{2} \int_0^{2\pi} d\phi_k \int_0^{2\pi} d\phi_{k'} (\mathbf{k} - \mathbf{k}')^2 u[\cos(\phi_k - \phi_{k'})]. \end{aligned} \quad (\text{A5})$$

<sup>1</sup>P. M. Solomon, P. J. Price, D. J. Frank, and D. C. La Tulipe, Phys. Rev. Lett. **63**, 2508 (1989).

<sup>2</sup>T. J. Gramila, J. P. Eisenstein, A. H. MacDonald, L. N. Pfeiffer, and K. W. West, Phys. Rev. Lett. **66**, 1216 (1991); Surf. Sci.

**263**, 446 (1992).

<sup>3</sup>T. J. Gramila, J. P. Eisenstein, A. H. MacDonald, L. N. Pfeiffer, and K. W. West, Phys. Rev. B **47**, 12957 (1993).

<sup>4</sup>H. Rubel, E. H. Linfield, D. A. Ritchie, K. M. Brown, M. Pepper,

- and G. A. C. Jones, *Semicond. Sci. Technol.* **10**, 1229 (1995).
- <sup>5</sup>H. Noh, S. Zelakiewicz, T. J. Gramila, L. N. Pfeiffer, and K. W. West, *Phys. Rev. B* **59**, 13114 (1999).
- <sup>6</sup>M. Kellogg, J. P. Eisenstein, L. N. Pfeiffer, and K. W. West, *Solid State Commun.* **123**, 515 (2002).
- <sup>7</sup>C. Jörger, S. J. Cheng, H. Rubel, W. Dietsche, R. Gerhardt, P. Specht, K. Eberl, and K. v. Klitzing, *Phys. Rev. B* **62**, 1572 (2000).
- <sup>8</sup>R. Pillarisetty, H. Noh, D. C. Tsui, E. P. De Poortere, E. Tutuc, and M. Shayegan, *Phys. Rev. Lett.* **89**, 016805 (2002).
- <sup>9</sup>U. Sivan, P. M. Solomon, and H. Shtrikman, *Phys. Rev. Lett.* **68**, 1196 (1992).
- <sup>10</sup>R. Rubel, A. Fisher, W. Dietsche, C. Jörger, K. von Klitzing, and K. Eberl, *Physica E (Amsterdam)* **1**, 160 (1997).
- <sup>11</sup>N. P. R. Hill, J. T. Nicholls, E. H. Linfield, M. Pepper, D. A. Ritchie, A. R. Hamilton, and G. A. C. Jones, *J. Phys.: Condens. Matter* **8**, L557 (1996); H. Rubel, A. Fischer, W. Dietsche, K. von Klitzing, and K. Eberl, *Phys. Rev. Lett.* **78**, 1763 (1997); X. G. Feng, S. Zelakiewicz, H. Noh, T. J. Ragucci, T. J. Gramila, L. N. Pfeiffer, and K. W. West, *ibid.* **81**, 3219 (1998); C. Jörger, W. Dietsche, W. Wegscheider, and K. von Klitzing, *Physica E (Amsterdam)* **6**, 586 (2000).
- <sup>12</sup>M. B. Pogrebinskii, *Fiz. Tekh. Poluprovodn. (S.-Peterburg)* **11**, 637 (1977) [*Sov. Phys. Semicond.* **11**, 372 (1977)].
- <sup>13</sup>P. J. Price, *Physica B & C* **117/118**, 750 (1983).
- <sup>14</sup>K. Flensberg and Ben Yu-Kuang Hu, *Phys. Rev. Lett.* **73**, 3572 (1994); *Phys. Rev. B* **52**, 14796 (1995).
- <sup>15</sup>N. P. R. Hill, J. T. Nicholls, E. H. Linfield, M. Pepper, D. A. Ritchie, G. A. C. Jones, Ben Yu-Kuang Hu, and K. Flensberg, *Phys. Rev. Lett.* **78**, 2204 (1997); N. P. R. Hill, J. T. Nicholls, E. H. Linfield, M. Pepper, D. A. Ritchie, Ben Yu-Kuang Hu, and K. Flensberg, *Physica B* **249–251**, 868 (1998).
- <sup>16</sup>H. Noh, S. Zelakiewicz, X. G. Feng, T. J. Gramila, L. N. Pfeiffer, and K. W. West, *Phys. Rev. B* **58**, 12621 (1998).
- <sup>17</sup>M. V. Fischetti and S. E. Laux, *J. Appl. Phys.* **89**, 1205 (2001).
- <sup>18</sup>M. V. Fischetti, *J. Appl. Phys.* **89**, 1232 (2001).
- <sup>19</sup>P. M. Solomon and Min Yang, *IEEE Electron Devices Meeting*
- <sup>20</sup>S. M. Sze, *Physics of Semiconductor Devices* (Wiley, New York, 1981).
- <sup>21</sup>*Numerical Data and Functional Relationships in Science and Technology*, edited by O. Madelung, M. Schulz, and H. Weiss, Landolt-Börnstein, New Series, Group III, Vol. 17, Pt. a (Springer, New York, 1982).
- <sup>22</sup>P. M. Solomon and B. Laikhtman, *Superlattices Microstruct.* **10**, 89 (1991).
- <sup>23</sup>B. Laikhtman and P. M. Solomon, *Phys. Rev. B* **41**, 9921 (1990); A.-P. Jauho and H. Smith, *ibid.* **47**, 4420 (1993); A. Yurtsever, V. Moldoveanu, and B. Tanatar, *Solid State Commun.* **125**, 575 (2003).
- <sup>24</sup>D. L. Maslov, *Phys. Rev. B* **45**, 1911 (1992).
- <sup>25</sup>M. Mosko, V. Cambel, and A. Moskova, *Phys. Rev. B* **46**, 5012 (1992); V. Cambel and M. Mosko, *Semicond. Sci. Technol.* **8**, 364 (1993).
- <sup>26</sup>H. C. Tso, P. Vasilopoulos, and F. M. Peeters, *Phys. Rev. Lett.* **68**, 2516 (1992).
- <sup>27</sup>I. I. Boiko, P. Vasilopoulos, and Yu. M. Sirenko, *Phys. Rev. B* **45**, 13538 (1992).
- <sup>28</sup>A.-P. Jauho and H. Smith, *Phys. Rev. B* **47**, 4420 (1993).
- <sup>29</sup>L. Zheng and A. H. MacDonald, *Phys. Rev. B* **48**, 8203 (1993).
- <sup>30</sup>A. Kamenev and Y. Oreg, *Phys. Rev. B* **52**, 7516 (1995).
- <sup>31</sup>K. Flensberg, Ben Yu-Kuang Hu, A.-P. Jauho, and J. M. Kinaret, *Phys. Rev. B* **52**, 14761 (1995).
- <sup>32</sup>H. C. Tso, P. Vasilopoulos, and F. M. Peeters, *Phys. Rev. Lett.* **70**, 2146 (1993).
- <sup>33</sup>L. Swierkowski, J. Szymanski, and Z. W. Gortel, *Phys. Rev. Lett.* **74**, 3245 (1995); *Phys. Rev. B* **55**, 2280 (1997).
- <sup>34</sup>A. Yurtsever, V. Moldoveanu, and B. Tanatar, *Solid State Commun.* **125**, 575 (2003).
- <sup>35</sup>H. L. Cui, X. L. Lei, and N. J. M. Horing, *Superlattices Microstruct.* **13**, 221 (1993).
- <sup>36</sup>V. F. Gantmakher and Y. B. Levinson, *Carrier Scattering in Metals and Semiconductors* (North-Holland, Amsterdam, 1987).
- <sup>37</sup>C. A. Neugebauer, *J. Appl. Phys.* **39**, 3177 (1968); T. I. Kamins, *ibid.* **42**, 4365 (1971); J. Y. W. Seto, *ibid.* **46**, 5247 (1975); G. Baccarani, B. Ricco, and G. Spadini, *ibid.* **49**, 5565 (1978); J. Levinson, F. R. Shepherd, P. J. Scanlon, W. D. Westwood, G. Este, and M. Rider, *ibid.* **53**, 1193 (1982).
- <sup>38</sup>T. Ando, A. B. Fowler, and F. Stern, *Rev. Mod. Phys.* **54**, 437 (1982).
- <sup>39</sup>M. Chr. Bonsager, K. Flensberg, Ben Yu-Kuang Hu, and A. H. MacDonald, *Phys. Rev. B* **57**, 7085 (1998).
- <sup>40</sup>F. F. Fang and W. E. Howard, *Phys. Rev. Lett.* **16**, 797 (1966).
- <sup>41</sup>G. F. Giuliani and J. J. Quinn, *Phys. Rev. B* **26**, 4421 (1982).
- <sup>42</sup>S. T. Pantelides and C. T. Sah, *Phys. Rev. B* **10**, 621 (1974).
- <sup>43</sup>G. D. Wilk, R. M. Wallace, and J. M. Anthony, *J. Appl. Phys.* **89**, 5243 (2001).